The effects of geometric detail on the vibratory responses of complex ship-like thin-walled structures

Apostolos Grammatikopoulos

Maritime Engineering Group, University of Southampton, Boldrewood Innovation Campus, Burgess Rd, SO17 6QF Southampton, United Kingdom

Abstract

Hydroelasticity of ships and studies in coupled antisymmetric vibrations have become increasingly important with container ships becoming faster and more slender. In this investigation, a ship-like structure is modelled and an equivalent backbone with a U-shaped cross section is designed. Their responses are compared, and limitations of various modelling approaches are discussed. It is demonstrated that scaling of the natural frequencies is insufficient to ensure scaling of the antisymmetric mode shapes and the relevant differences are quantified. Consequently, the backbone model should be viewed as a separate structure for validation purposes rather than a scaled model of a ship.

Keywords: cellular, geometric detail, modal testing, prismatic beam structures, structural vibrations, thin-walled hull girders

1. Introduction

Hydroelasticity of ships, a term that describes the strong coupling between the hydrodynamic loads from the sea surface and the vibratory responses of the vessel, has become an increasingly important subject with ships growing longer and faster [1]. The area was introduced in the 1970s [2] and quickly evolved from 2D potential flow methods to 3D potential flow [3] and 3D RANS [4]. From a structural perspective, ships tend to be modelled as beams, due to their length being much larger than their other dimensions [5]. Some investigations use shell elements instead [6], but this approach has been less popular when coupled with RANS, due to the increased computational cost.

Models for hydroelastic experiments tend to separate the hydrodynamic and structural aspects. Accordingly, a rigid model of the hull is split into segments and then the flexibility is provided by a flexible backbone [7] or, more rarely, a series of flexible joints between segments [8]. There have been very few models with a ship-shaped structure, also acting as the hydrodynamic boundary, primarily due to the increased complexity and cost associated with them [9, 10, 11, 12].

Numerous models have been manufactured to measure the symmetric vibratory responses of ships, usually featuring a backbone with a rectangular, box-shaped cross section. It can be proven that, for these models, scaling of the bending stiffness is sufficient to ensure scaling of the natural frequencies, the strains and, consequently, structural loads. There have been far fewer cases of models for measurement of antisymmetric responses.

One of the few experiments in antisymmetric responses was presented by Hong et al., who used a model with an H-shaped backbone to investigate the vibrations a large container ship [13]. This is a most unusual choice, as the centroid and shear centre of such a backbone are coincident, unlike the full-scale vessel. The open section of the model allowed appropriate scaling of 1$^{\text{st}}$ symmetric and antisymmetric natural frequencies, but no coupling between horizontal bending and torsion was present, so the relevant

Email address: A.Grammatikopoulos@soton.ac.uk (Apostolos Grammatikopoulos)

modes would appear separately. Kim et al. improved this model by replacing the H-shaped backbone with a U-shaped backbone [14]. The 1st antisymmetric natural frequency, in model scale, was approximately 78% of the 1st symmetric. However, in this publication the shear centre location is presented only for the backbone and not for the full-scale vessel. The authors demonstrated that torsional moments are significantly different between the H-shaped backbone, where antisymmetric mode coupling is ignored, and the U-shaped backbone. Finally, Hong & Kim measured higher order resonant symmetric and antisymmetric responses of this model, as well as transient symmetric responses [13].

Iijima et al. argued that box-shaped and channel cross sections for the backbone result in too high and too low torsional stiffness, respectively, and suggested box-shaped bacbones with a few deck openings [15]. Their design procedure was based on scaling of the bending/torsional stiffness and corresponding natural frequencies. Zhu et al. [16] used a box-shaped backbone with a few openings at the top, emulating the ship's deck openings, to investigate responses in horizontal bending and torsion. Five openings were manufactured, which only spanned a small part of the length of the backbone. Consequently, the 1st antisymmetric natural frequency, scaled up, was 91% of the 1st symmetric. The 1st antisymmetric natural frequency would have actually been much higher, had the authors not lowered it through the ballast distribution. When the model was placed in water, the added mass effects affected its symmetric natural frequencies much more than the antisymmetric, resulting in a 1st antisymmetric natural frequency 6.5% higher than the 1st symmetric. The mode shapes for deflection and internal loads were compared to those predicted by computational models of the backbone. Following research by the authors focused on the hydrodynamic effects of an increased bow flare [17].

Marón & Kapsenberg also manufactured a similar backbone but, in this case, the deck openings spanned more than half of the backbone length [18]. The resulting 1st antisymmetric natural frequency was approximately 55% of the 1st symmetric. The authors provided an extensive discussion on best practice when designing and manufacturing a model for hydroelastic experiments.

Storhaug et al. [19] used a segmented model of a 13000 TEU container ship, in which the segments were linked using flexible joints rather than a backbone. This arrangement has the advantage of controlling the natural frequencies with ease. In this case, the 1st antisymmetric natural frequency in full scale was approximately 81% of the 1st symmetric. The authors claim that the sophisticated flexible joints used allowed scaling of the coupled natural frequencies as well. However, it is unclear whether the joints actually imposed any coupling between horizontal bending and torsion, which is generally the main drawback stemming from the artificial nature of such a connection. Despite scaling the antisymmetric natural frequencies, the investigation subsequently focused on transient symmetric responses, rendering this issue less important.

Houtani et al. manufactured an elastic model of a container ship to measure symmetric and antisymmetric vibrations [11]. The model comprised an external shell of polymer foam with the shape of the ship. By making the load-bearing structure the size of the entire model, the authors managed to have a shear centre below the bottom of the vessel, something that could not be achieved with a backbone model. In fact, the achieved distance between the centroid and the shear centre was only 3% different than their target. The 1st antisymmetric natural frequency, in model scale, was approximately 94% of the 1st symmetric.

Grammatikopoulos et al. [20] developed a method to design and manufacture elastic models, including significant structural detail, using additive manufacturing. The produced methodology was shown to accurately predict the natural frequencies of such a model, including up to the 5th antisymmetric mode, after which there were no experimental results to compare to the simulations. In this case, the 1st antisymmetric natural frequency, in model scale, was approximately 87% of the 1st symmetric for a model not including any ballast. Symmetric responses of this model in waves were measured [12] but experiments on antisymmetric responses have not been published yet. The model was not based on an existing ship but on a vessel from a benchmark study on a small container ship [10].

A few conclusions can be easily drawn from the above. Firstly, the publications on antisymmetric responses of ships are limited and the models manufactured for this purpose are even fewer. This is not due to a lack of interest in the subject, as the extensive literature on relevant computational methods demonstrates. The primary issues are, instead, the difficulty in desiging and manufacturing appropriate models, the need for specialised expertise combining structural dynamics, applied mechanics, material science, and hydrodynamics in an experimental and computational environment, and the need for an ocean basin to measure the hydroelastic responses, which is not available in many institutions worldwide. More importantly, within this small pool of work, investigators tend to verify that their models represent the ships they are trying to emulate by checking only the scaling of the natural frequencies. In some cases, comparison of experimental measurements and simulation results for the mode shapes of the scaled model is performed, but the mode shapes of the scaled model are not compared to the mode shapes of the full-scale ship. Although this is probably sufficient when modelling symmetric responses, antisymmetric responses are significantly affected by the coupling between horizontal bending and torsion, which is also discussed in the work of Hirdaris et al. [1]. As demonstrated above, particularly with examples such as the H-shaped backbone, scaling the natural frequencies does not ensure the correct level of coupling or even any coupling at all.

This investigation looks into the vibratory responses of a ship-like structure and an equivalent U-shaped backbone. In section 2 the finite element modelling procedure is described and the backbone is designed so that its first three natural frequencies are identical to that of the ship. In this sense, it follows the typical design procedure for backbone models. No scaling is used, as the results are not compared to experimental measurements, and a backbone with the same length as the ship is designed instead. In section 4 the natural frequencies beyond the first three are compared and the differences between mode shapes are quantified. In section 5 the accuracy of modelling both structures as beams is evaluated by comparing to shell modelling. Limitations of the various approaches are thoroughly discussed. In section 6 it is demonstrated that backbone models can be insufficient to emulate the antisymmetric responses of ships, even if several natural frequencies are accurately scaled. Recommendations are provided for future investigations, including best practice for backbone models, and prompts for the exploration of models with a more geometrically accurate structure.

2. Finite element modelling

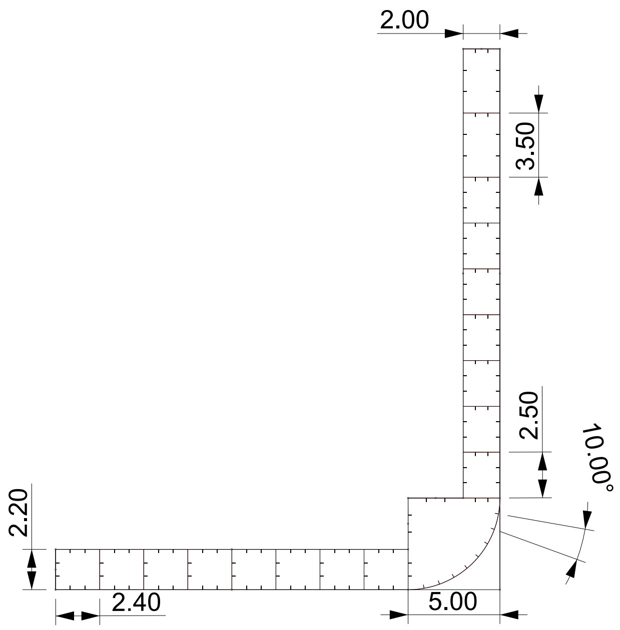

Figure 1: Dimensions of various structural details of the ship's cross section. All stiffeners split the corresponding plates into equal segments and had a width of 0.2 m. The two top cells of the double side have a different height than the bottom cells. All thickness, including plating and stiffeners, were equal to 0.02 m.

Four models were produced in ANSYS Mechanical APDL for this study, consisting of the combinations of two geometries and two modelling techniques. The two structures were a prismatic ship-like structure, hereafter referred to as the *ship*, and a channel section representing an equivalent backbone that could be used in a segmented model, hereafter referred to as the *backbone*. The two modelling techniques differed in the type of element used, namely shell elements or beam elements that included warping responses. Details for all the models are summarised in Table 1. A target mesh size of 0.2 m was used for all models. The cross section of the ship, including dimensions for all structural detail, is depicted in Figure 1.

Table 1: A summary of the parameters corresponding to each of the models. The density of the backbone was calculated to produce the same mass as the ship. All models share the same length and target element size. The geometric parameters were shared for models of the same structure. The vertical locations of the centroid and shear centre were measured from the bottom of the respective model.

Model name	Ship, shell	Ship, beam	Backbone, shell	Backbone, beam
Element type	SHELL181 [21]	BEAM188 [22]	SHELL181 [21]	BEAM188 [22]
Number of elements	4,481,924	1,760	411,840	1,760
Mass (kg)	1.7653E+07	1.7110E+07	1.7653E+07	1.7653E+08
Structure	Ship		Backbone	
Target element size (m)	0.2		0.2	
Density (kg/m^3)	7700		1713.22	
Young's modulus (N/m^2)	200E9		200E9	
Poisson's ratio	0.3		0.3	
Length (m)	350		350	
Breadth (m)	48.4		20.4	
Depth (m)	29.5		12.8	
Thickness (m)	0.02		0.64	
Sectional area (m^2)	6.473	6.349	29.440	
2$^{\text{nd}}$ moment of area, y-axis (m^4)	562.63	552.64	522.22	
2$^{\text{nd}}$ moment of area, z-axis (m^4)	2346.1	2396.1	2159.3	
Torsion constant (m^4)		20.565	4.067	
Warping constant (m^6)		197,490	38,059	
Centroid vertical location (m)	9.0660	9.2451	3.8795	
Shear centre vertical location (m)		-10.112	-4.7160	
Vertical shear area coefficient	0.24308		0.35847	
Transverse shear area coefficient	0.25931		0.38825	

The *ship shell element model* was the most general and complex model generated. It was modelled as shell elements with a uniform thickness of 0.02 m. The cross section was inspired by the container ship used by Senjanović et al. [23], with slightly changed dimensions. The dimensions of different aspects of the cross section are depicted in detail in Figure 1. To simplify comparison between models and as this study did not focus on the effects of stiffness distribution, a constant cross section was used throughout; 19 equally spaced bulkheads were included, and deep frames were added halfway between pairs of consecutive bulkheads. To facilitate comparison to beam models by having a uniform mass distribution, both bulkheads and deep frames were modelled as massless, although their stiffness and Poisson's ratio were the same as for the rest of the structure, a modelling technique that has been previously used, for example, for a bulk carrier [3], and a passenger ship [6]. The mesh of this model is shown in Figure 2. The high accuracy of this method has also been previously demonstrated through comparison to experimental results on a different vessel [20].

The *ship beam element model* replicated the model above while using beam elements that included warping responses. The cross section was generated in the form of a 2D surface and meshed within ANSYS as a custom beam section. The bulkheads and stiffeners were not modelled individually. The sectional properties were calculated by ANSYS as slightly different (approximately 1-2%) to the ones calculated in CAD, that were considered to correspond to the ship shell model. This was attributed to differences between modelling the surface in CAD and within ANSYS APDL. Consequently, the mass of the model was approximately 3% smaller to that of the ship shell model.

The *backbone shell element model* was generated following the frequency-matching method: the dimensions of the cross section were iterated to match the first natural frequency, then the first and the second at

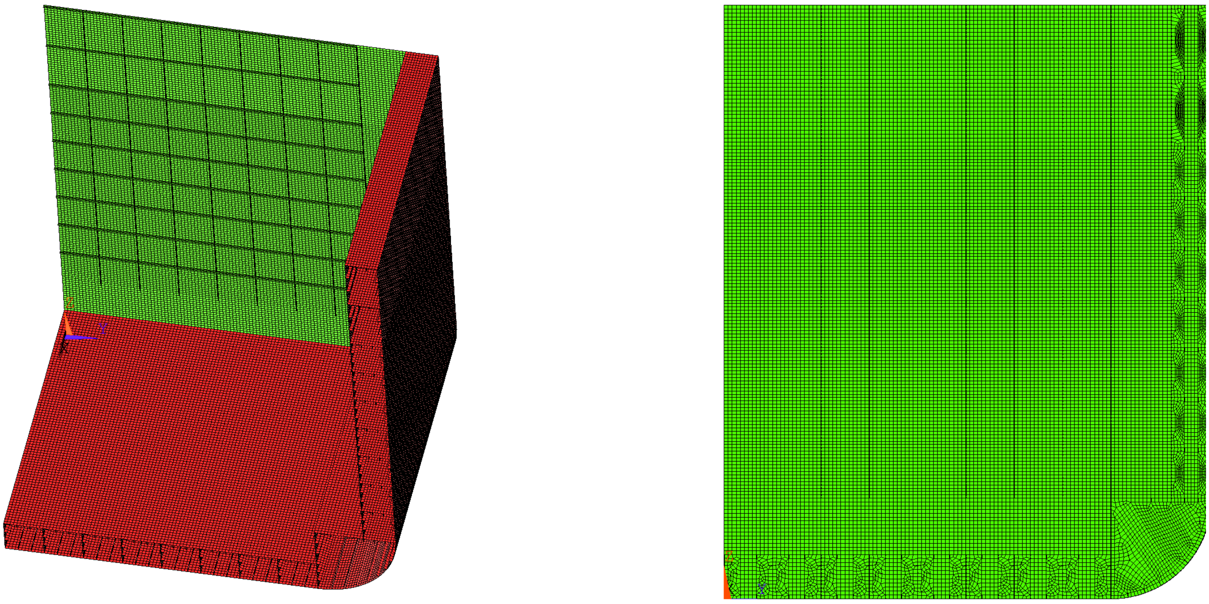

(a) Birdseye view (b) Bulkhead

Figure 2: Mesh of the ship shell element model. The bulkhead elements in green are massless but otherwise share the same Young's modulus and Poisson's ratio as the remaining structure. The bulkhead is only stiffened in its central part where the unsupported length is large, to avoid contamination with local modes. The length of the depicted in subfigure (a) corresponds to the length between two consecutive bulkheads and includes one deep frame halfway through.

the same time, and finally the first three natural frequencies at the same time (Figure 3). A symmetric channel (U-shaped) cross section was generated with uniform thickness, and the breadth, depth and thickness were modified in an iterative manner until the first three natural frequencies matched the ones predicted by the ship shell element model within 0.5%. In all cases, the density of the backbone was modified so that its mass was equal to that of the ship. This ensured that all differences observed in the responses stemmed entirely from the stiffness characteristics of the structure rather than its inertia and facilitated the comparison of results.

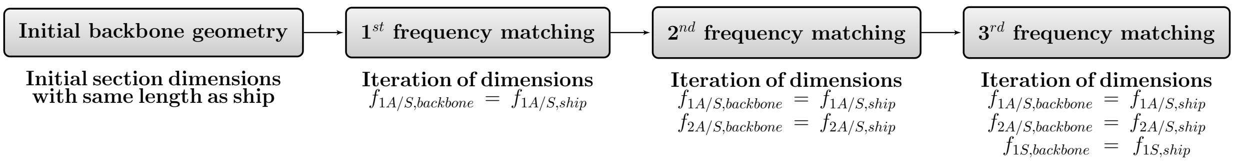

Figure 3: Flowchart of the procedure to design the backbone model. The initial dimensions of the cross section were arbitrarily selected, and then iterated until the 1^{st} antisymmetric natural frequency was matched. In the following steps, the iterative geometry changes were smaller, aiming to gradually match more frequencies. A tolerance of 0.5% was allowed when comparing natural frequencies.

The *backbone beam element model* replicated the model above while using beam elements that included warping responses. It used a built-in channel cross section that already existed in ANSYS and the density was calculated in the same manner as for the backbone shell element model.

The significantly lower density used for the backbone models might seem like an unnatural decision at first, despite its practical advantages. In reality though, the mass of the structure of the ship, that was calculated for the ship shell element model, would only be a small portion of the total mass of vessel. Most mass contributions would originate from machinery, cargo and consumables. For this size of container ship, it expected that the light ship, that is the mass of the ship without any cargo, crew, or consumables, is approximately 20% of the mass at full load condition. The mass of the ship structure is only a fraction of this. When scaled physical models of ships are produced for hydroelastic experiments, the combined mass of the backbone and segments tends to be larger than the mass of a scaled ship structure would be, but that only means that there is less need for additional "ballast" masses to emulate the correct mass distribution (for example [24, 25]). Another approach would be to include additional masses representing machinery, cargo and consumables in all models. However, this would provide no further insight regarding mode shape similarity and would thus be beyond the scope of this study.

The mesh size was selected to ensure convergence of the ship shell element model. Then the same sizing was used for the other models, despite being finer than necessary, to allow direct comparison of the same positions along the length for the various mode shapes. A structured mesh, that is a a mesh with orthogonal quadrilateral elements, was used for the central part of the bulkheads and all the longitudinal structure of the vessel. Free meshing was used for the remaining part of the bulkheads (see Figure 2).

The Block Lanczos eigenvalue extraction method [26] was the solver used. The block shifted Lanczos algorithm is a variation of the classical Lanczos algorithm, where the Lanczos recursions are performed using a block of vectors, as opposed to a single vector. Comparison of natural frequencies between the mesh used and one with double the size produced a difference of 0.02% for the 6^{th} natural frequency, corresponding to the 3-node vertical bending mode, and much smaller differences for all other frequencies, ensuring mesh convergence.

3. Natural frequency comparison

A summary of the natural frequencies calculated using each of the structural models is presented in Table 2. The shell element model of the ship was considered to be the most general and the frequencies it predicted were used as a benchmark. The percentage of difference between the results from the other three models and the ship shell element model is depicted in Figure 4.

Table 2: Natural frequencies for the first six modes, as predicted by the various models. A/S stands for antisymmetric and S stands for symmetric. The number of nodes for each mode shape is provided in a separate column. Full description of the mode shapes, in order of appearance: (a) 1-node torsion (b) 2-node horizontal bending - 2-node torsion (c) 2-node vertical bending (d) 3-node horizontal bending - 3-node torsion (e) 2-node horizontal bending - 2-node torsion (f) 3-node vertical bending.

Mode		# Nodes	Predicted frequency			
			Ship		Backbone	
			shell	beam	shell	beam
1^{st}	A/S	1	0.3923	0.4054	0.3929	0.4055
2^{nd}	A/S	2	1.0109	1.0380	1.0161	1.0308
1^{st}	S	2	1.3037	1.3059	1.3039	1.3104
3^{rd}	A/S	3	2.3199	2.4161	2.3911	2.4895
4^{th}	A/S	2	3.0956	3.1938	3.5095	3.5831
2^{nd}	S	3	3.1844	3.2278	3.2397	3.5416

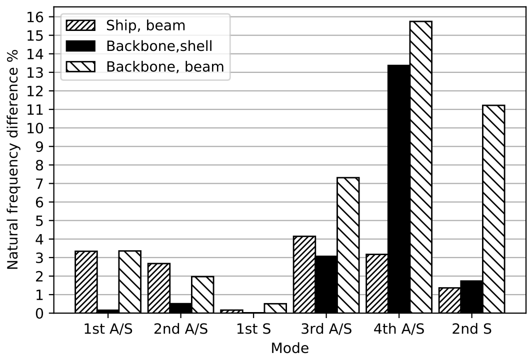

Figure 4: Difference in percentage of the natural frequencies predicted by various models compared to the frequencies predicted by the ship shell element model.

The ship beam element model produced uniformly higher natural frequencies than its shell element counterpart. The differences ranged between approximately 1% and 4% and can be partly attributed to the small differences in mass between the two models.

The backbone shell element model was designed to match the first three natural frequencies of the ship shell element model, so it should come as no surprise that the relevant differences are less than 0.5%. Slightly larger differences were observed for the 3-node horizontal bending - 3-node torsional mode (3^{rd} antisymmetric) at approximately 3% and the 3-node vertical bending mode (2^{nd} symmetric). The second

2-node horizontal bending - 2-node torsional natural frequency was more than 13% higher for the backbone shell element model.

The backbone beam element model produced relatively inconsistent results, with some natural frequencies being very close to the benchmark and the remaining featuring moderate to large differences, up to 16%. The pattern follows, to some extent, that of the backbone shell model, with the 2nd antisymmetric and the 1st symmetric natural frequencies being very close to the target and larger differences observed for the 3rd and, even more so, the 4th antisymmetric modes. Interestingly though, the 1st antisymmetric and the 2nd symmetric natural frequencies are very dissimilar to the results from both the ship shell element model and the backbone shell element model. The results for the 1st antisymmetric mode are almost identical, in fact, to those produced by the ship beam element model. Potential origins of these discrepancies will be discussed in Section 5.

4. Mode shape depiction & comparison

In order to perform quantitative comparison of the mode shapes from different modelling techniques, it was necessary to generated a depiction of the shell mode shapes in a manner compatible with the beam mode shapes, that is a 1-D depiction of the structure. With that in mind, the average displacements and rotations at various cross sections along the length of the structure were obtained. For antisymmetric modes, the transverse displacement UY and the torsional rotation ROTX were depicted and the mode shapes were normalised for unit rotation at x=0. For symmetric modes, the vertical displacement UZ was depicted and normalised for unit displacement at x=0.

The mode shapes are depicted in Figures 5-10, with each figure corresponding to one mode. Different line types are used for each model, with the ship models being grouped in black colour and backbone models being grouped in red colour. For antisymmetric modes both translation along the Y-axis and rotation around the X-axis are depicted. For symmetric modes only translation along Z-axis is depicted.

5. Accuracy of beam approximation

Figures 5-10 demonstrate that shell and beam approximations for either type of structure produce very similar results. In most cases, the two approximations are within 10% and often within 3% of each other in terms of mode shapes. Symmetric mode shapes, in particular, have almost no difference at all. More significant differences were observed for the 1st and 4th antisymmetric modes. The end points of the 1st antisymmetric mode shape are 49% and 37% larger according to shell model predictions, compared to beam model predictions, for ship and backbone, respectively(Figure 11), agreeing with previous findings [27]. These figures reduce to 11% and 25% for the 4th antisymmetric mode (Figure 12).

The discrepancies in the 1st antisymmetric mode are particularly surprising, as it is the lowest mode of the structure overall, so accuracy would be expected to be high. It appears that beam modelling consistently underestimates the displacements near the ends of the structure, whether it is ship-shaped or backbone-shaped. The differences are concentrated around the quarter-lengths near the ends. These discrepancies are even more localised for the 4th antisymmetric mode, being significant only for approximately 10% of the length from either end. Considering that the areas of maximum strain for these two modes are at the midpoint and at quarter length from the ends, respectively, the effects of these differences are not expected to be overwhelming. In any case, the level of horizontal bending in the 1st antisymmetric mode, which is torsion-dominated, is sufficiently small that the differences due to beam modelling would not affect the shape significantly.

More alarming is the difference between the predicted natural frequencies for the 2nd symmetric mode shape of the backbone, as predicted by the corresponding shell and beam models. The average vertical translation of the backbone does not indicate any issues. Observing the three-dimensional mode shape (Figure 13) , however, reveals a mode shape that does not correspond to a beam structure, but is instead a 3-node vertical bending - 3-node in-plane shear mode [28].

It is evident from the above that in-plane shear is excited at similar frequencies as the beam-like modes of the backbone. Indeed, modal analysis of the cross section of the backbone in plane strain condition revealed

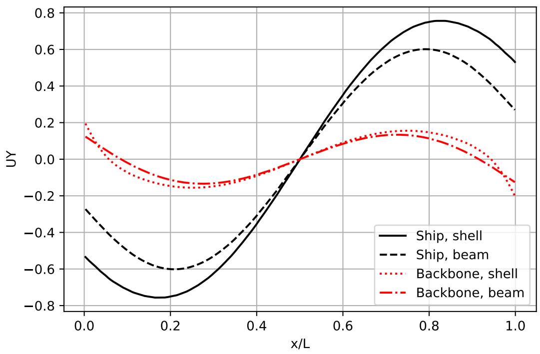

(a) Y translation

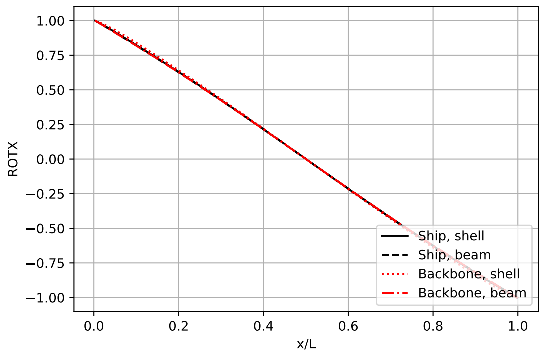

(b) X rotation

Figure 5: Results for the 1^{st} antisymmetric mode shape. All mode shapes have been normalised for unit rotation at x=0.

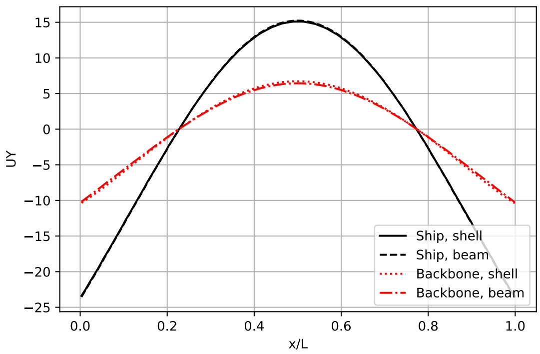

(a) Y translation

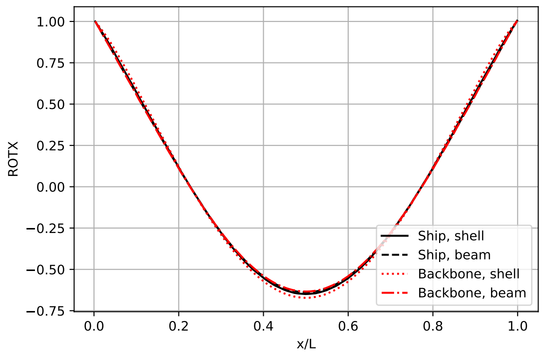

(b) X rotation

Figure 6: Results for the 2^{nd} antisymmetric mode shape. All mode shapes have been normalised for unit rotation at x=0.

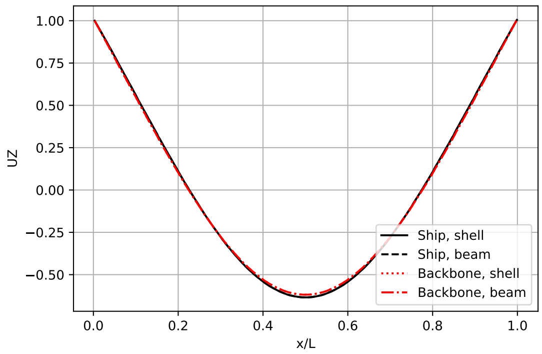

(a) Z translation

Figure 7: Results for the 1^{st} symmetric mode shape. All mode shapes have been normalised for unit translation at x=0.

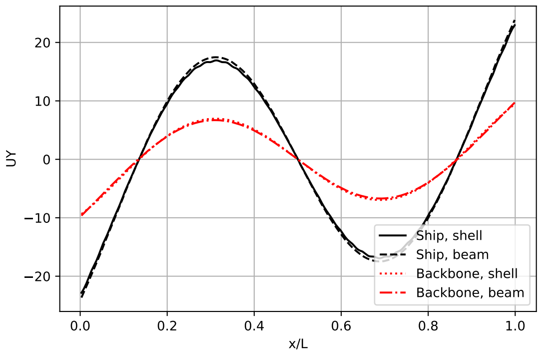

(a) Y translation

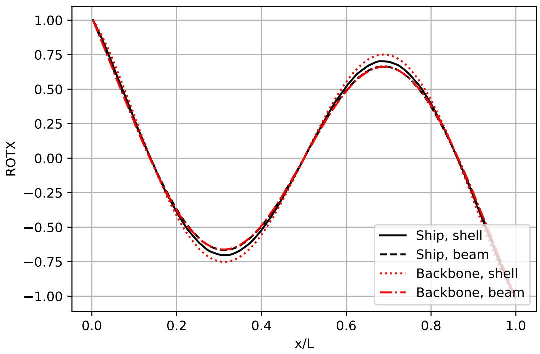

(b) X rotation

Figure 8: Results for the 3$^{\text{rd}}$ antisymmetric mode shape. All mode shapes have been normalised for unit rotation at x=0.

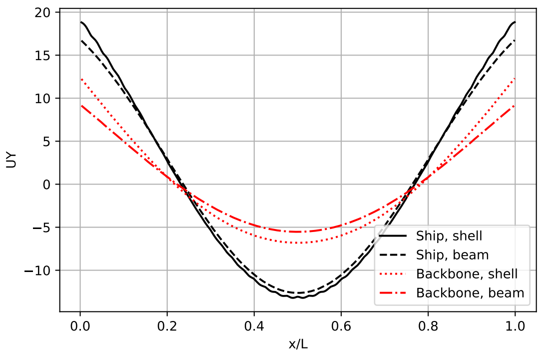

(a) Y translation

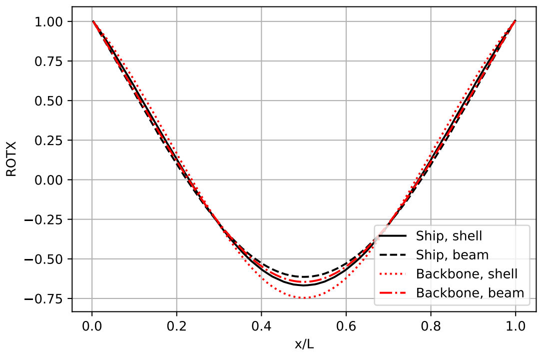

(b) X rotation

Figure 9: Results for the 4$^{\text{th}}$ antisymmetric mode shape. All mode shapes have been normalised for unit rotation at x=0.

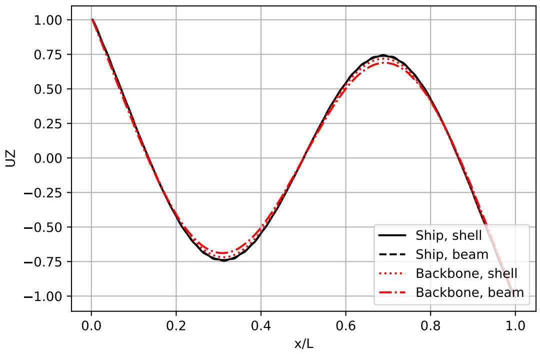

(a) Z translation

Figure 10: Results for the 2$^{\text{nd}}$ symmetric mode shape. All mode shapes have been normalised for unit translation at x=0.

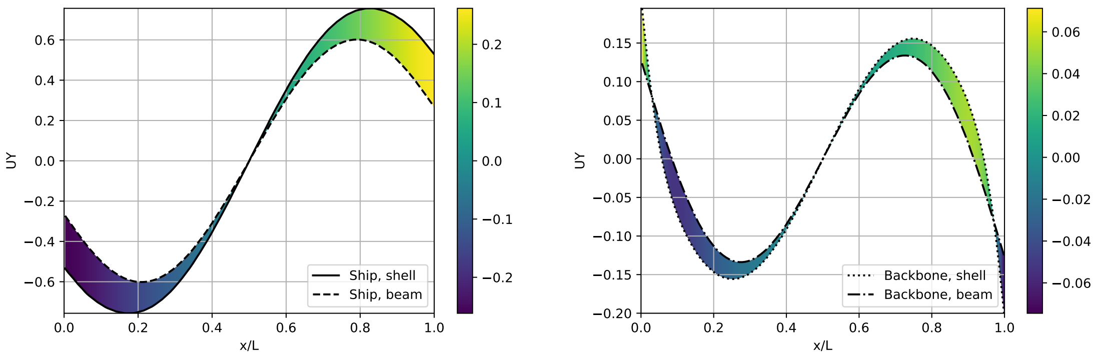

(a) Ship, Y translation

(b) Backbone, Y translation

Figure 11: Comparison between shell and beam results for the 1$^{\text{st}}$ antisymmetric mode shape Y translation.

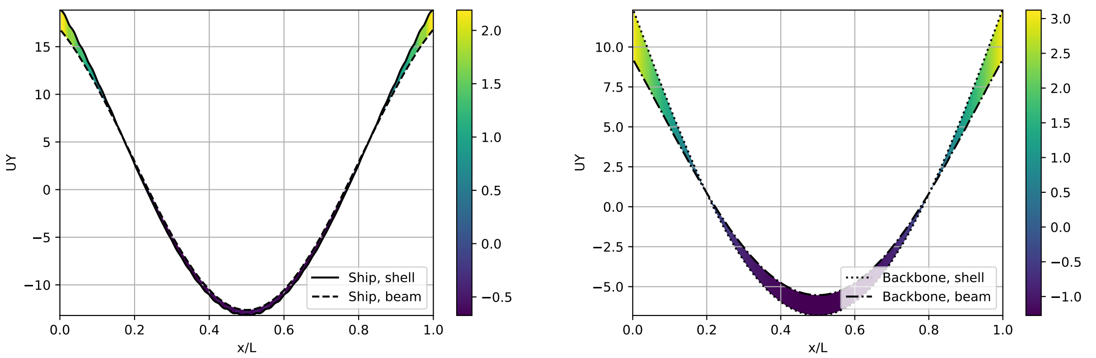

(a) Ship, Y translation

(b) Backbone, Y translation

Figure 12: Comparison between shell and beam results for the 4$^{\text{th}}$ antisymmetric mode shape Y translation. All mode shapes have been normalised for unit rotation at x=0.

that the natural frequency of the 1$^{\text{st}}$ in-plane mode is equal to 3.34 Hz. Performing the same analysis for the cross section of the ship, the 1$^{\text{st}}$ in-plane mode is excited at a natural frequency that is two orders of magnitude lower, at 0.063 Hz. The relevant mode shapes are depicted in Figure 14.

The extremely low in-plane shear natural frequency of the ship would be a significant problem, if the ship was a purely prismatic structure like the backbone. However, the ship features significant transverse stiffening through its numerous bulkheads and deep frames. The free length between each pair of subsequent transverse structural components is sufficiently short to suppress the in-plane modes.

The above suggests that transverse reinforcement of the backbone at regular intervals would allow suppression of these undesired responses. The simplest implementation of this is through the use of backbones with deck openings rather than channel-shaped backbones. However, in order to achieve a 1$^{\text{st}}$ antisymmetric natural frequency that is significantly lower than the 1$^{\text{st}}$ symmetric natural frequency, the openings would have to take up most of the length of the backbone, as seen in the work by Marón & Kapsenberg [18].

In order to test this assumption, the cross section of the backbone shell model was closed at the longitudinal location of every bulkhead, by adding a 0.6 m-wide strip of material at the top. The result was a series of 0.6 m long closed box-shaped sections, in between the 20 segments of open channel sections. These strips, similarly to the bulkheads, shared the same stiffness and Poisson's ratio as the rest of the material but were massless, to retain the uniform mass distribution of the backbone. In any case,their small size meant that, even if their mass was included, the dynamic response of the structure would not be significantly affected. The natural frequencies of the resulting shell model are compared to those of the backbone shell and beam element models in Table 3. Most of the natural frequencies remain almost unchanged compared

(a) Side view

(b) Top view

Figure 13: The 2$^{\text{nd}}$ symmetric mode shape of the backbone, when modelled with shell elements, no longer corresponds to the response of a beam.

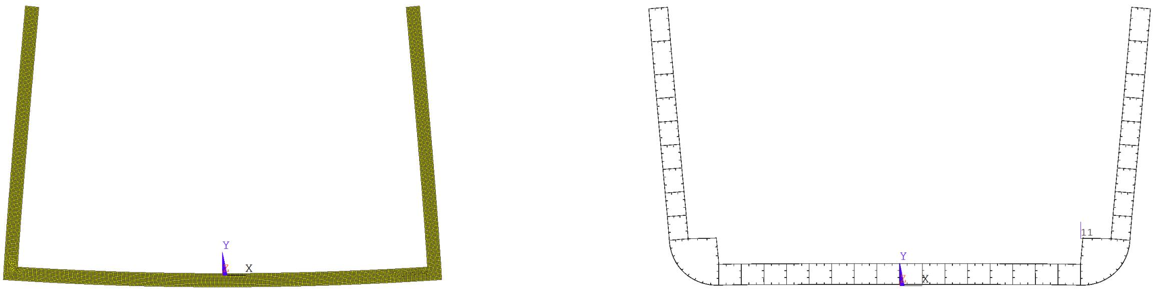

(a) Backbone section

(b) Ship section

Figure 14: The 1$^{\text{st}}$ in-plane shear mode of the cross sections of the backbone, at 3.34 Hz and of the ship, at 0.063 Hz, assuming plane strain condition.

to the original backbone shell model, with the exception of the 2$^{\text{nd}}$ symmetric natural frequency, where the in-plane aspects have been suppressed and the results agree well with the beam model (Figure 15).

Table 3: Comparison of the predicted natural frequencies of the backbone shell element model, the backbone beam element model, and the modified shell element model where the backbone had transverse reinforcements. A/S stands for antisymmetric and S stands for symmetric. The number of nodes for each mode shape is provided in a separate column.

Mode		# Nodes	Predicted frequency		
			Shell	Beam	Modified shell
1$^{\text{st}}$	A/S	1	0.3929	0.4055	0.3970
2$^{\text{nd}}$	A/S	2	1.0161	1.0308	1.0189
1$^{\text{st}}$	S	2	1.3039	1.3104	1.307
3$^{\text{rd}}$	A/S	3	2.3911	2.4895	2.399
4$^{\text{th}}$	A/S	2	3.5095	3.5831	3.516
2$^{\text{nd}}$	S	3	3.2397	3.5416	3.489

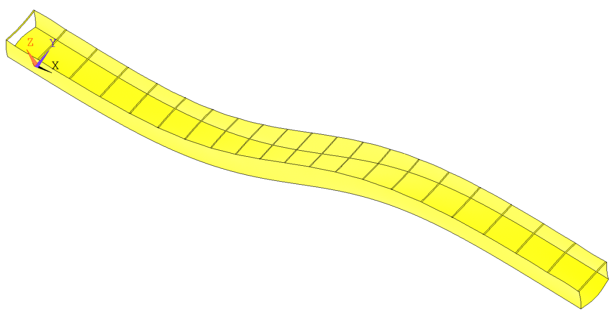

Figure 15: The narrow strips at the bulkhead locations provided enough transverse reinforcement to the backbone to eliminate any in-plane shear.

In summary, the differences between beam and shell results in terms of antisymmetric modes shapes should not be disregarded and are particularly pronounced for the 1$^{\text{st}}$ antisymmetric mode. The natural frequencies present some discrepancies, increasingly so for higher modes. These differences, however, do not exceed 4% and in many cases are below 1%, with the exception of the 2$^{\text{nd}}$ symmetric mode, which was found to be contaminated with in-plane shear responses. Minimal transverse support, in the form of thin strips, resolved that problem altogether.

6. Comparison between ship structure and equivalent backbone

The comparison between the antisymmetric modes of the ship shell element model and the backbone shell element model is summarised in Figure 16. The differences between the two models are much larger than the ones observed when comparing shell and beam modelling. Namely, the difference between the two models at the ends of the 1st, 2nd, 3rd and 4th antisymmetric modes was equal to 136%, 56%, 59% and 35%, respectively. These large discrepancies were due to the significant difference in distance between the centroid and the shear centre of the corresponding cross sections.

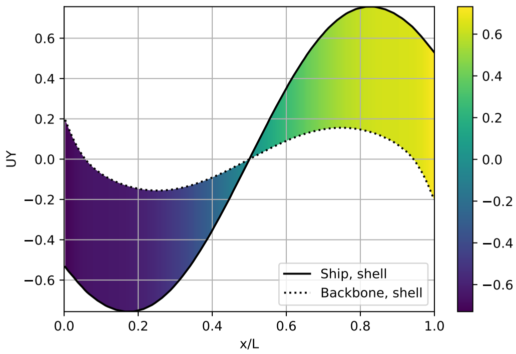

(a) 1st A/S mode, Y translation

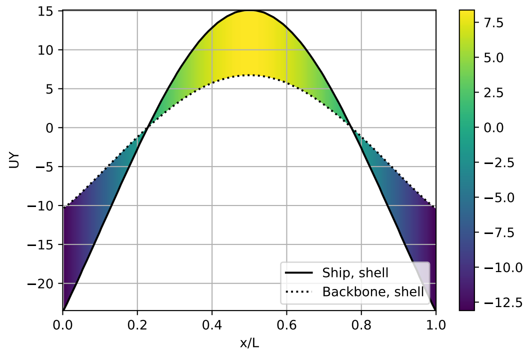

(b) 2nd A/S mode, Y translation

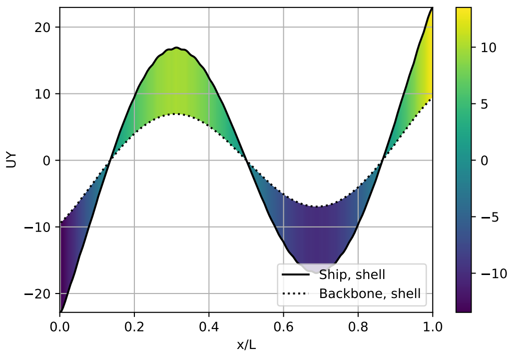

(c) 3rd A/S mode, translation

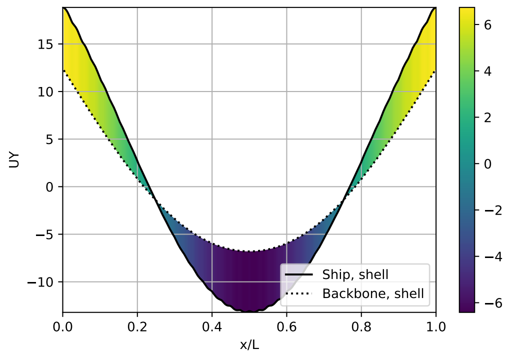

(d) 4th A/S mode, Y translation

Figure 16: Comparison between ship and backbone shell models' results for the antisymmetric mode shape Y translation. All mode shapes have been normalised for unit rotation at x=0.

A comparison of internal loads, namely bending moment and shear force distribution, for all antisymmetric modes, is summarised in Table 4. Since the differences between ship and backbone for each mode were significantly larger than those between shell and beam approximations, it was decided that the comparison of internal load results, produced using the beam models, was valid. As the shape of the distributions was very similar for both models, the comparison between the two structures is performed using the ratio between the maximum torsional moment and the corresponding maximum horizontal bending moment.

Table 4: The ratio of the maximum torsional moment over the maximum horizontal bending moment for each of the antisymmetric mode shapes of the ship and backbone structures.

A/S Mode	Torsional Moment / Bending moment ratio	
	Ship	Backbone
1st	22.541	22.732
2nd	0.335	0.154
3rd	0.762	0.369
4th	0.037	0.014

The ratio between the two moments was found to be less than 1% different for the 1st antisymmetric mode, which is torsion-dominated. However, for all the other antisymmetric modes, where horizontal bending is more pronounced, the ship's bending moment compared to its torsional moment was more than double of what was observed for the backbone. This difference resulted from the significantly higher levels of horizontal bending for the same angle of torsion (Figure 16).

The large differences in mode shapes will significantly alter the deformed shape of the hull while excited by beam or oblique seas and, consequently, hinder the accurate calculation of hydrodynamic loads. The same level of torsion on the hull causes increased horizontal bending responses on the real ship compared to the backbone, and vice versa. Although experiments with such models can be used, to some extent, to validate computational codes, it should be clear that the backbone model does not necessarily represent the responses of the ship. It would be unwise to scale the results up; separate simulations would have to be run to calculate the loads and responses of the real vessel.

7. Conclusions

Hydroelastic experiments for ships are performed mostly using backbone models. The backbones for container ships tend to have either a constant, U-shaped cross section or a box-shaped cross section with deck openings. In this manner, the location of the shear centre is moved below the bottom of the cross section, but still not at the correct distance from the centroid.

In this investigation it was confirmed that beam approximation produces slightly different results than the shell formulation, but the differences are not sufficiently large to invalidate the assumption that ships behave approximately like beams. It was demonstrated, however, that prismatic U-shaped backbones are prone to in-plane shear responses that can contaminate mode shapes of interest. These in-plane responses can severely affect both the corresponding natural frequencies and the accuracy of beam theory to describe their mode shapes and dynamic responses. Using closed section backbones with deck openings can overcome this issue, but the deck openings should span most of the length of the backbone if the 1$^{\text{st}}$ antisymmetric natural frequency of the ship is significantly lower than the 1$^{\text{st}}$ symmetric.

Furthermore, it was demonstrated that the antisymmetric mode shapes of a backbone can differ significantly from those of the vessel, even if several natural frequencies are matched during design. Differences in the mode shapes for deflection and internal loads lead to incorrect coupling between horizontal bending and torsion. Consequently, the results from backbone models do not necessarily represent the responses of the real vessels, even if the natural frequencies are scaled accurately.

It is recommended that future investigations do not only present the achieved natural frequencies in their findings. Comparison of the mode shapes of the full-scale vessel and the model-scale backbone should be performed as well and, in cases of large discrepancies, it should be emphasised that the results only apply to the model. Codes validated using these results can then be used for separate simulations to identify the responses of the real ship.

This work should be expanded in the future through experimental modal analysis of geometrically detailed models of ships, for the identification of not only beam-like modes but also in-plane shear modes. Development of experimental procedures that allow investigators to rigorously decompose their models' modes and safeguard against contamination is imperative. Use of techniques that obtain deformation fields instead of point accelerations might be necessary to achieve this.

Acknowledgements

The author acknowledges the use of the IRIDIS High Performance Computing Facility, and associated support services at the University of Southampton, in the completion of this work. The author would like to thank J.M.F.A. Blanchard for the invaluable feedback on this manuscript.

References

[1] S. E. Hirdaris and P. Temarel, "Hydroelasticity of ships: Recent advances and future trends," *Journal of Engineering for the Maritime Environment*, vol. 223, no. 3, pp. 305–330, 2009.

[2] R. E. D. Bishop and W. G. Price, *Hydroelasticity of ships.* Cambridge University Press, 1979.

[3] S. E. Hirdaris, G. W. Price, and P. Temarel, "Two- and three-dimensional hydroelastic modelling of a bulker in regular waves," *Marine Structures*, vol. 16, no. 8, pp. 627–658, 2003.

[4] P. A. Lakshmynarayanana and S. Hirdaris, "Comparison of nonlinear one- and two-way FFSI methods for the prediction of the symmetric response of a containership in waves," *Ocean Engineering*, vol. 203, no. January, p. 107179, 2020.

[5] I. Senjanović, I. Ćatipović, and S. Tomašević, "Coupled flexural and torsional vibrations of ship-like girders," *Thin-Walled Structures*, vol. 45, no. 12, pp. 1002–1021, 2007.

[6] J. Tilander, M. Patey, and S. Hirdaris, "Springing analysis of a passenger ship in waves," *Journal of Marine Science and Engineering*, vol. 8, no. 7, 2020.

[7] N. Fonseca and C. Guedes Soares, "Experimental investigation of the nonlinear effects on the vertical motions and loads of a containership in regular waves," *Journal of Ship Research*, vol. 48, no. 2, pp. 118–147, 2004.

[8] J. Lavroff, M. R. Davis, D. S. Holloway, and G. A. Thomas, "Wave slamming loads on wave-piercer catamarans operating at high-speed determined by hydro-elastic segmented model experiments," *Marine Structures*, vol. 33, pp. 120–142, 2013.

[9] I. Watanabe, M. Ueno, and H. Sawada, "Effects of Bow Flare Shape to the Wave Loads of a container ship," *Journal of the Society of Naval Architects of Japan*, vol. 1989, no. 166, pp. 259–266, 1989.

[10] Y.-S. Wu, R.-Z. Chen, and J.-R. Lin, "Experimental technique of hydroelastic ship model," in *Proceedings of the Third International Conference on Hydroelasticity, Oxford, UK, September*, pp. 15–17, 2003.

[11] H. Houtani, Y. Komoriyama, S. Matsui, M. Oka, H. Sawada, Y. Tanaka, and K. Tanizawa, "Designing a hydro-structural model ship to experimentally measure its vertical-bending and torsional vibrations," in *8th International Conference on Hydroelasticity in Marine Technology*, (Seoul, Korea), 2018.

[12] A. Grammatikopoulos, J. Banks, and P. Temarel, "Experimental hydroelastic responses of an elastic container ship-inspired barge model produced using additive manufacturing," in *8th International Conference on Hydroelasticity in Marine Technology*, (Seoul, Korea), pp. 75–84, 2018.

[13] S. Y. Hong and B. W. Kim, "Experimental investigations of higher-order springing and whipping-WILS project," *International Journal of Naval Architecture and Ocean Engineering*, vol. 6, pp. 1160–1181, 2014.

[14] B. W. Kim, K.-H. Kim, Y. S. Kim, and S. Y. Hong, "Torsion Moment Conversion Methods in Model Test With U-shape Backbone," in *Proceedings of the Twenty-fourth (2014) International Ocean and Polar Engineering Conference*, pp. 782–791, 2014.

[15] K. Iijima, O. A. Hermundstad, S. Zhu, and T. Moan, "Symmetric and antisymmetric vibrations of a hydroelastically scaled model," in *Proceedings of the 5th International Conference on Hydroelasticity in Marine Technology*, vol. 1213796053, 2009.

[16] S. Zhu, M. Wu, and T. Moan, "Experimental investigation of hull girder vibrations of a flexible backbone model in bending and torsion," *Applied Ocean Research*, vol. 33, no. 4, pp. 252–274, 2011.

[17] S. Zhu and T. Moan, "A comparative study of the influence of bow shape on hull girder vibrations through two backbone models," in *Proceedings of the 6th International Conference on Hydroelasticity in Marine Technology*, no. 1251, (Tokyo, Japan), pp. 153–162, 2012.

[18] A. Marón and G. K. Kapsenberg, "Design of a ship model for hydro-elastic experiments in waves," *International Journal of Naval Architecture and Ocean Engineering*, vol. 6, pp. 1130–1147, jan 2014.

[19] G. Storhaug, Q. Derbanne, B.-K. Choi, T. Moan, and O. A. Hermundstad, "Effect of Whipping on Fatigue and Extreme Loading of a 13000Teu Container Vessel in Bow Quartering Seas Based on Model Tests," in *Proceedings of the 30th International Conference on Ocean, Offshore and Arctic Engineering*, (Rotterdam, The Netherlands), pp. 1–10, 2011.

[20] A. Grammatikopoulos, J. Banks, and P. Temarel, "Prediction of the vibratory properties of ship models with realistic structural configurations produced using additive manufacturing," *Marine Structures*, vol. 73, 2020.

[21] K.-J. Bathe and E. N. Dvorkin, "A formulation of general shell elements—the use of mixed interpolation of tensorial components," *International journal for numerical methods in engineering*, vol. 22, no. 3, pp. 697–722, 1986.

[22] J. C. Simo and L. Vu-Quoc, "A three-dimensional finite-strain rod model. part ii: Computational aspects," *Computer methods in applied mechanics and engineering*, vol. 58, no. 1, pp. 79–116, 1986.

[23] I. Senjanović, S. Tomašević, and N. Vladimir, "An advanced theory of thin-walled girders with application to ship vibrations," *Marine Structures*, vol. 22, no. 3, pp. 387–437, 2009.

[24] G. Storhaug, *Experimental investigation of wave induced vibrations and their effect on the fatigue loading of ships.* PhD thesis, 2007.

[25] S. S. Denchfield, *An Investigation into the Influence of Rogue Waves on a Traveling Ship.* PhD thesis, Faculty of Engineering, Science and Mathematics School of Engineering Sciences, 2011.

[26] R. G. Grimes, J. G. Lewis, and H. D. Simon, "A shifted block lanczos algorithm for solving sparse symmetric generalized eigenproblems," *SIAM Journal on Matrix Analysis and Applications*, vol. 15, no. 1, pp. 228–272, 1994.

[27] S. E. Hirdaris, S. H. Miao, and P. Temarel, "The effect of structural discontinuity on antisymmetric response of a container ship," *In Proceedings of the 5th International Conference on Hydroelasticity in Marine Technology, Southampton, UK*, pp. 57–68, 2009.

[28] S. Ádány, "Decomposition of in-plane shear in thin-walled members," *Thin-Walled Structures*, vol. 73, pp. 27–38, 2013.